Energy Localization Using Anisotropic Left-Handed Materials

Guan Xia Yu[a], Xin Ye Yu[b], Li Juan Xia[c], and Bai Bing Xv[c]

[a] School of Science, Nanjing Forestry University, Nanjing 210037, P. R. China.
[b] Jiangsu Provincial Zhenjiang No.1 High school, Zhenjiang 212004, P. R. China.
[c] College of Information Science and Technology, Nanjing Forestry University, Nanjing 210037, P. R. China.

Reprint requests to G. X. Y.; E-mail: sys@njfu.com.cn

Z. Naturforsch. **68a,** 300 – 304 (2013) / DOI: 10.5560/ZNA.2012-0119
Received May 15, 2012 / revised October 21, 2012 / published online February 20, 2013

A theoretical analysis of the phenomena of electromagnetic (EM) energy localization is presented for an anisotropic left-handed material (ALHM) slab. If the EM parameters of the transverse magnetic (TM) modes in the ALHM slab satisfy $\varepsilon_y/\varepsilon_z = 1$, $\mu_x\varepsilon_z = \mu_0\varepsilon_0$, the EM energy localization can be realized between two sources located at two sides of the ALHM slab. This could be proven by theoretical analysis and numerical simulations in this paper.

Key words: Electromagnetic Energy Localization; Anisotropic Left-Handed Materials.
PACS numbers: 41.20.JB; 78.20.Ci; 42.25.Bs; 84.40.Az

1. Introduction

Recently, the novel properties of metamaterials have attracted considerable attention of many researchers in various fields [1 – 7]. One type of metamaterial is the left-handed material (LHM), which was proposed by Veselago forty years ago [1]. Since the LHM has negative electromagnetic parameters, this feature gives rise to the negative refractive index and the backward-wave propagation. In other words, the wave vector k forms a left-handed triplet with the vectors E and H, and the wave fronts for propagating waves travel towards the source, opposite to the direction of energy flow. At that time, these materials did not draw too much attention until the negative refraction index could be realized by man-made structures below the electromagnetic plasma frequency [3, 4]. In recent years, many artificial materials with positive or negative electromagnetic parameters have been explored [8], and many other novel phenomena have been discovered theoretically [9 – 15].

The localization of the electromagnetic energy is one of the novel properties of the LHM [11, 12]. If two sources with opposite current directions were placed at the perfect-imaging points of the LHM slab, all electromagnetic energies could be localized in a small region completely between the two sources. This is because the electromagnetic waves are completely counterbalanced outside two sources due to the two opposite current sources. As the localized modes are of high quality, the localization of electromagnetic waves could find applications in a variety of optical and microwave devices, such as narrow-band filters and low-threshold lasers.

Because the man-made materials are always anisotropic and lossy [16 – 20], it is difficult to synthesize the ideal isotropic LHM. Actually, to our knowledge, the isotropic LHMs have not been prepared successfully in experiments for the time being. Therefore, it is interesting to investigate whether the localization of electromagnetic energy based on isotropic LHMs can still be generated or not in the anisotropic LHM (ALHM). In this paper, the characteristics of electromagnetic (EM) fields in the ALHM are discussed firstly, then the different conditions of super imaging using the ALHM slab have been illustrated. Secondly, in order to realize energy localization, the special EM parameters in the ALHM slab are obtained. Thirdly, numerical simulations of EM energy localization have been carried out, which are in conformity with theoretical analysis.

2. Theoretical Analysis

The geometrical structure under consideration is shown in Figure 1. The slab located at $z = d_1$ and

$z = d_2$ is filled with an anisotropic LHM, which separates the whole space into three regions. The two semi-infinite regions (Region 0, $z < d_1$ and Region 2, $z > d_2$) are occupied by free space with the relative permittivity $\varepsilon_{r_0} = \varepsilon_{r_2} = 1$ and the relative permeability $\mu_{r_0} = \mu_{r_2} = 1$. The slab (Region 1, $d_1 < z < d_2$) is an anisotropic LHM with relative permittivity tensor $\bar{\varepsilon}_{r_1}$ and relative permeability tensor $\bar{\mu}_{r_1}$. Taken the optical axis as z axial, the relative permittivity $\bar{\varepsilon}_{r_1}$ and relative permeability $\bar{\mu}_{r_1}$ are denoted as

$$\bar{\varepsilon}_{r_1} = (\varepsilon_{r_x}, \varepsilon_{r_y}, \varepsilon_{r_z}), \quad \bar{\mu}_{r_1} = (\mu_{r_x}, \mu_{r_y}, \mu_{r_z}).$$

Suppose that a three-dimensional vertical electric dipole source (VED) was located at the origin of the Cartesian coordinate system along $+z$ direction in the region 0, it would generate the electromagnetic waves of TM-mode. In this system, the z-components of the electromagnetic field in the three regions can be written in the following form:

$$E_{iz} = -\frac{Il}{4\pi\omega\varepsilon_0}\int_0^\infty \mathrm{d}k_\rho \frac{k_\rho^3}{k_{0z}} J_0^{(1)}(k_\rho \rho)\,\tilde{E}_{iz}, \qquad (1)$$

where Il is the momentum of the dipole, and k_ρ is the wave vector along longitude. $\tilde{E}_{iz}$ corresponds to spectral components in the three different regions (Fig. 1), which can be written as

$$\tilde{E}_{0z} = \mathrm{e}^{\mathrm{i}k_{0z}|z|} + R\,\mathrm{e}^{-\mathrm{i}k_{0z}z}, \quad z < d_1, \qquad (2)$$

$$\tilde{E}_{1z} = C^+\,\mathrm{e}^{\mathrm{i}k_{1z}z} + C^-\,\mathrm{e}^{-\mathrm{i}k_{1z}z}, \quad d_1 < z < d_2, \qquad (3)$$

$$\tilde{E}_{2z} = T\,\mathrm{e}^{-\mathrm{i}k_{0z}z}, \quad z > d_2, \qquad (4)$$

in which k_0 is the wave vector in Region 0. k_{0z} and k_{1z} are the transverse wave numbers in Regions 0 and 1, which satisfy the different dispersion relations

$$k_{0z}^2 = k_0^2 - k_\rho^2, \qquad k_{1z}^2 = \omega^2\varepsilon_y\mu_x - \frac{\varepsilon_y}{\varepsilon_z}k_\rho^2. \qquad (5)$$

R and T are the reflection and transmission coefficients in Region 0 and 2, C^+ and C^- represent the component coefficients transmitted forward and backward in Region 1. The unknown coefficients in (2)–(4) can be determined by the boundary conditions

$$R = (p_{12}^2 - p_{11}^2)\,\mathrm{e}^{2\mathrm{i}k_{0z}d_1} \cdot (\mathrm{e}^{\mathrm{i}k_{1z}(d_2-d_1)} - \mathrm{e}^{-\mathrm{i}k_{1z}(d_2-d_1)})/D, \qquad (6)$$

$$C^+ = -2(p_{12} - p_{11})\,\mathrm{e}^{\mathrm{i}k_{0z}(d_3-d_2)}\,\mathrm{e}^{-\mathrm{i}k_{1z}d_2}/D, \qquad (7)$$

$$C^- = 2(p_{12} + p_{11})\,\mathrm{e}^{\mathrm{i}k_{1z}d_1}\,\mathrm{e}^{-\mathrm{i}k_{0z}(d_3-d_2)}/D, \qquad (8)$$

$$T = -4p_{11}p_{12}\,\mathrm{e}^{\mathrm{i}k_{0z}(d_3-d_2+d_1)}/D, \qquad (9)$$

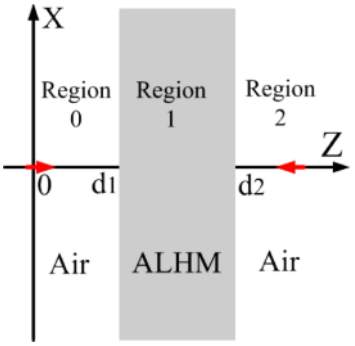

Fig. 1 (colour online). The whole space is divided in three regions by a ALHM slab located between $z = d_1$ and $z = d_2$, and two electric dipoles are sited at image points.

where $p_{11} = \varepsilon_z k_{1z}/\varepsilon_y k_{0z}$ and $p_{12} = \varepsilon_z/\varepsilon_0$. D is the denominator written as

$$D = (p_{12} - p_{11})^2\,\mathrm{e}^{\mathrm{i}k_{1z}(d_2-d_1)} - (p_{12} + p_{11})^2\,\mathrm{e}^{\mathrm{i}k_{1z}(d_1-d_2)}. \qquad (10)$$

In (1), the fields in the three regions are only determined by three electromagnetic parameters ε_{r_y}, ε_{r_z}, and μ_{r_x}, and other relative electromagnetic parameters can be regarded as 1. If we consider $\varepsilon_{r_y} = \varepsilon_{r_z} = \mu_{r_x} = -1$, we have $k_{0z} = -k_{1z}$, $R = 0$, and $T = \mathrm{e}^{-\mathrm{i}4k_{oz}d_1}$, which means the results are the same as in the case of an isotropic LHM slab [3]. In this case, there should be two symmetrical imaging positions. One imaging is at $z = 2d_1$ within the slab, the other is at $z = 4d_1$ in Region 2. If another three-dimensional VED point source with opposite current direction is placed at the perfect-imaging points $z = 4d_1$, all electromagnetic energies could be localized in a small region completely between the two sources. The electromagnetic waves are completely counterbalanced outside the two sources due to the two opposite current sources [11, 12].

For the sake of realizing the electromagnetic energy localization, the conditions of perfect imaging are necessary. In (6)–(9), if $p_{11} = p_{12}$ and $k_{1z} < 0$, it is easy to attain $R = 0$ and $T = \mathrm{e}^{-2\mathrm{i}(k_{oz}-k_{1z})(d_1-d_2)}$, which means there should be two perfect imaging points. However, we note that the field in Region 2 is different from the case of the isotropic LHM. The amplitude in the anisotropic LHM slab is proportional to p_{11} (8), which is determined by different choices of electromagnetic parameters. According to (5)–(10), two cases are considered to realize perfect imaging.

Firstly, if ε_{r_y}, ε_{r_z}, and μ_{r_x} are all less than zero and satisfy $\varepsilon_y\varepsilon_z = \varepsilon_0^2$, $\mu_x\varepsilon_z = \mu_0\varepsilon_0$, the perfect imag-

ing conditions can be acquired easily. We get $k_{1z}^2 = -\varepsilon_y/\varepsilon_z k_{0z}^2$, $p_{11} = p_{12} = \sqrt{\frac{\varepsilon_z}{\varepsilon_y}}$, which is not the same as with isotropic LHMs. In this case, although two images can be focused in Region 1 and Region 2, the imaging positions are not symmetrically. If $\varepsilon_y/\varepsilon_z < 1$, then $|k_{1z}| < k_{0z}$, the imaging position in the ALHM is larger than $2d_1$, which deviates from symmetrical imaging positions (Fig. 2a). In addition, since the amplitude of the field in Region 1 is related to p_{11} (8), the amplitude of the transmitting waves in Region 1 should be increased, and should be larger than the amplitude in Region 0 and 2. If $\varepsilon_y/\varepsilon_z > 1$, then $|k_{1z}| > k_{0z}$, the imaging position in the ALHM is less than $2d_1$ (Fig. 2b), and the amplitude of the transmitting waves in Region 1 should be decreased, and should be less than the amplitude in Region 0 and 2. Therefore, in this case, if another three-dimensional VED point source with opposite current direction is placed at the perfect-imaging points $z = 4d_1$, the electromagnetic energies can not be completely counterbalanced outside the two sources, and the localization of the electromagnetic energy can not be achieved between the two sources.

Secondly, if ε_{r_y}, ε_{r_z}, and μ_{r_x} are all less than zero and satisfy $\varepsilon_y/\varepsilon_z = 1$, $\mu_x\varepsilon_z = \mu_0\varepsilon_0$, then $|k_{1z}| = k_{0z}$, which means that the wave vectors of the tangential component and the radial component are all continuous among the three regions. Therefore, there are two symmetrical images in Region 1 and Region 2, respectively. Figure 3a shows the distribution of the electric fields E_z along the z-direction for $\varepsilon_{r_y} = \varepsilon_{r_z} = -0.8$ and $\mu_{r_x} = -1.25$; the other conditions are the same (Fig. 2). Two symmetrical images are focused at $z = 0.8$ m in Region 1 and $z = 1.6$ m in Re-

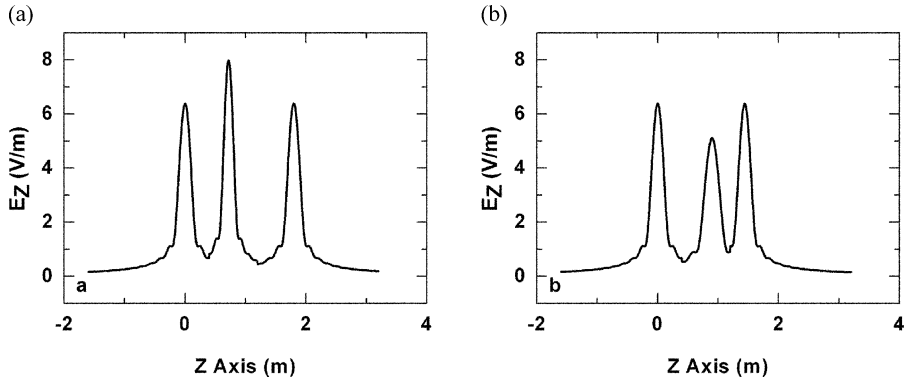

Fig. 2. Distribution of the electric field of E_z along the z-direction with $x = 0$, where a ALHM is located between $z_1 = 0.4$ m and $z_2 = 1.2$ m, and a 3-VED point source with $IL = 1$ A m and $f = 1$ GHz is localized at $z = 0$. (a) $\varepsilon_{r_y} = -1.25$, $\varepsilon_{r_z} = -0.8$, and $\mu_{r_x} = -1.25$ in Region 1. (b) $\varepsilon_{r_y} = -0.8$, $\varepsilon_{r_z} = -1.25$, and $\mu_{r_x} = -0.8$.

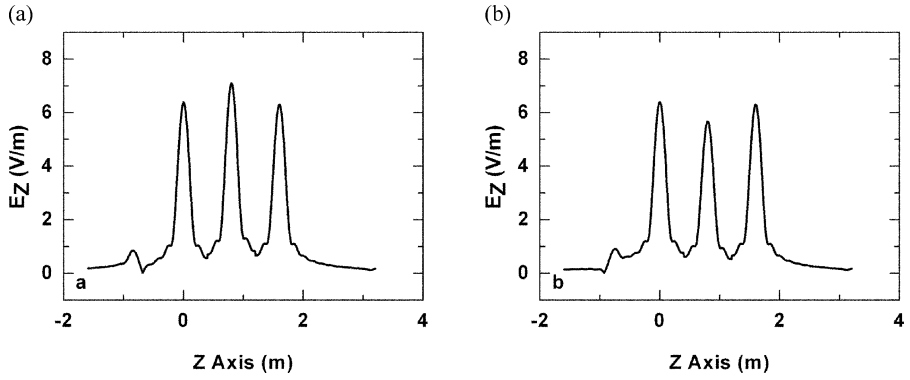

Fig. 3. Distribution of the electric field of E_z along the z-direction with $x = 0$, where a ALHM is located between $z_1 = 0.4$ m and $z_2 = 1.2$ m, and a 3-VED point source with $IL = 1$ A m and $f = 1$ GHz is localized at $z = 0$. (a) $\varepsilon_{r_y} = -0.8$, $\varepsilon_{r_z} = -0.8$, and $\mu_{r_x} = -1.25$ in Region 1. (b) $\varepsilon_{r_y} = -1.25$, $\varepsilon_{r_z} = -1.25$, and $\mu_{r_x} = -0.8$.

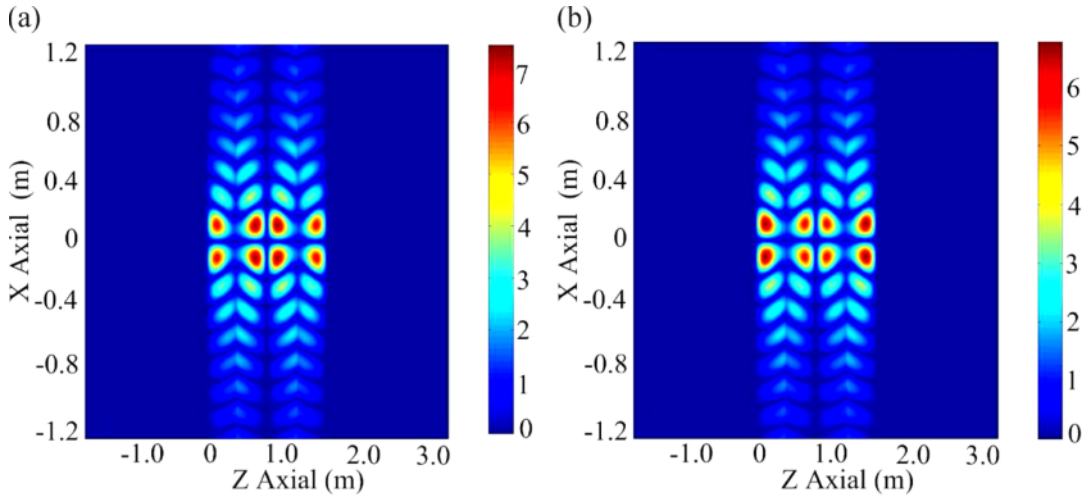

Fig. 4 (colour online). Distribution of the electric field of E_z along the z-direction, where two z-directed electric dipoles with opposite current directions are placed at the image points outside of the ALHM slab. The slab is located between $z_1 = 0.4$ m and $z_2 = 1.2$ m, and two 3-VED point sources with opposite directions are localized at $z = 0$ and $z = 1.6$ m. (a) $\varepsilon_{r_y} = -0.8$, $\varepsilon_{r_z} = -0.8$, and $\mu_{r_x} = -1.25$ in Region 1. (b) $\varepsilon_{r_y} = -1.25$, $\varepsilon_{r_z} = -1.25$, and $\mu_{r_x} = -0.8$.

gion 2, respectively. In addition, based on (10), D is in relation to $p_{12} = \varepsilon_z/\varepsilon_0$. When $\varepsilon_z < \varepsilon_0$, the maximum amplitude of the fields in Region 1 is less than that in Regions 0 and 2 (Fig. 3a). When $\varepsilon_{r_y} = \varepsilon_{r_z} = -0.8$ and $\mu_{r_x} = -1.25$, there are also two symmetrical images focused at Region 1 and Region 2, and the maximum amplitude of the fields in Region 1 is larger than that in Regions 0 and 2 (Fig. 3b). In this case, if another three-dimensional VED point source with opposite current direction is placed at the perfect-imaging points in Region 2, the electromagnetic energies can be completely counterbalanced out-

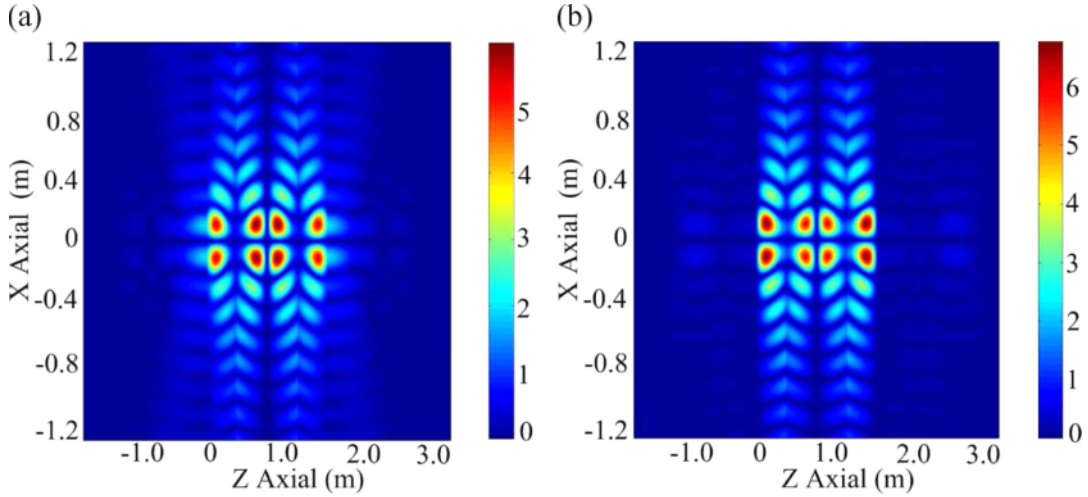

Fig. 5 (colour online). Distribution of the electric field of E_z along the z-direction, where two z-directed electric dipoles with opposite current directions are placed at the image points outside of the ALHM slab. The slab is located between $z_1 = 0.4$ m and $z_2 = 1.2$ m, and two 3-VED point sources with opposite directions are localized at $z = 0$ and $z = 1.6$ m. (a) $\varepsilon_{r_y} = -0.8 + \mathrm{i} \cdot 10^{-2}$, $\varepsilon_{r_z} = -0.8 + \mathrm{i} \cdot 10^{-2}$, and $\mu_{r_x} = -1.25 + \mathrm{i} \cdot 10^{-2}$ in Region 1. (b) $\varepsilon_{r_y} = -1.25 + \mathrm{i} \cdot 10^{-2}$, $\varepsilon_{r_z} = -1.25 + \mathrm{i} \cdot 10^{-2}$, and $\mu_{r_x} = -0.8 + \mathrm{i} \cdot 10^{-2}$.

side the two sources and are confined between the two sources.

3. Numerical Simulations

In order to validate the energy localization using the ALHM, full-wave numerical simulations have been carried out. An ALHM slab is located between $z = d_1 = 0.4\,\mathrm{m}$ and $z = d_2 = 1.2\,\mathrm{m}$, and two three-dimensional VED point sources $Il = 1\,\mathrm{mA}\cdot\mathrm{m}$ along the z-direction are located at the origin and at $z = 1.6\,\mathrm{m}$ with the opposite directions (Fig. 1), respectively. We consider that the frequencies of the two VED point sources are both 1 GHz.

According to the analysis above, firstly, we choose $\varepsilon_{r_y} = \varepsilon_{r_z} = -0.8$ and $\mu_{r_x} = -1.25$. The distribution of the electric field of E_z is shown in Figure 4a, from which we can see that the waves are all confined between the two sources. Due to $\varepsilon_{r_z} < \varepsilon_0$, the amplitude of the electromagnetic field in the center region is larger than that in the edge region, which is in line with the result of Figure 3a. Secondly, we choose $\varepsilon_{r_y} = \varepsilon_{r_z} = -1.25$ and $\mu_{r_x} = -0.8$. Figure 4b shows that the localization of the electromagnetic fields can also be achieved, and the amplitude of the electromagnetic field in the center region is smaller than that in the edge region due to $\varepsilon_{r_z} > \varepsilon_0$.

However, the man-made materials are always lossy more or less, therefore, it is difficult to make lossless artificial materials. The loss of the ALHM slab also has an influence on the electromagnetic energy localization. Due to the loss, the fields should be decreased along the direction of propagation, and the electromagnetic waves can not be completely counterbalanced outside the two sources. We choose $\varepsilon_{r_y} = \varepsilon_{r_z} = \varepsilon_{r1} + \mathrm{i}\varepsilon_{r2}$ and $\mu_{r_x} = \mu_{r_x1} + \mathrm{i}\mu_{r_x2}$, where ε_{r1} ε_{r2}, μ_{r_x1}, and μ_{r_x2} are real, and i is the imaginary unit. Figure 5 shows the distribution of the electric field of E_z with a weak lossy ALHM slab, where the little loss ($\varepsilon_{r2} = \mu_{r_x2} = 1\,\mathrm{e} - 3$) is considered; the other conditions are the same as in the lossless cases (Fig. 4). It is obvious that the electromagnetic fields are almost confined between the two sources for the little loss, though there are small leak of fields.

4. Conclusion

In this paper, the different electromagnetic parameters for choices of the perfect imaging and the energy localization are investigated theoretically in a ALHM slab. If the electromagnetic parameters of the TM mode in the ALHM slab satisfy $\varepsilon_y/\varepsilon_z = 1$, $\mu_x\varepsilon_z = \mu_0\varepsilon_0$, the EM energy localization can be realized between two three-dimensional VED point sources with opposite current directions located at the perfect-imaging points of both sides of the slab. Meanwhile, there are influences on the energy localization due to the loss of the ALHM slab. When there is a small loss in the ALHM slab, the energy localization can also be realized with several small leak of fields.

[1] V. G. Veselago, Sov. Phys. Usp. **10**, 509 (1968).
[2] J. B. Pendry, Phys. Rev. Lett **85**, 3966 (2000).
[3] D. R. Smith, W. J. Padilla, D. C. Vier, S. C. Nemat-Nasser, and S. Schultz , Phys. Rev. Lett. **84**, 4184 (2000).
[4] R. A. Shelby, D. R. Smith, and S. Schultz, Science **292**, 77 (2001).
[5] J. B. Pendry, D. Schurig, and D. R. Smith, Science **312**, 1780 (2006).
[6] D. Schurig, J. B. Pendry, and D. R. Smith, Opt. Express **14**, 9794 (2006).
[7] A. Alu, M. G. Silveirinha, A. Salandrino, and N. Engheta, Phys. Rev. B **75**, 155410 (2007).
[8] H. S. Chen, L. X. Ran, J. T. Huangfu, X. M. Zhang, and K. S. Chen, Phys. Rev. E **70**, 57605 (2004).
[9] R. Marco, A. C. Steven, D. Schurig, J. B. Pendry, and D. R. Smith, Phys. Rev. Lett. **100**, 63903 (2008).
[10] Y. Lai, J. Ng, H. Chen, D. Han, J. Xiao, Z. Q. Zhang, and C. T. Chan, Phys. Rev. Lett. **102**, 253902 (2009).
[11] Y. Lai, N. G. Jack, H. Y. Chen, Z. Q. Zhang, and C. T. Chen, Front. Phys. **5**, 308 (2010).
[12] H. Chen and C. T. Chan, Appl. Phys. Lett. **90**, 241105 (2007).
[13] Q. Cheng and T. J. Cui, Phys. Rev. B **72**, 113112 (2005).
[14] T. J. Cui, Q. Cheng, W. B. Lu, Q. Jiang, and J. A. Kong, Phy. Rev. B **71**, 45114 (2005).
[15] Q. Cheng and T. J. Cui, Opt. Lett. **30**, 1216 (2005).
[16] L. B. Hu and S. T. Chui, Phys. Rev. B **66**, 85108 (2002).
[17] R. Marques, F. Medina, and R. Rafii-El-Idrissi, Phys. Rev. B **65**, 144440 (2002).
[18] L. Yonghua, W. Pei, Y. Peijun, X. Jianping, and M. Hai, Opt. Commun. **246**, 429 (2005).
[19] A. V. Ivanov, O. A. Kotelnikova, and V. A. Ivanov, J. Magn. and Magn. Mate. **300**, 67 (2006).
[20] I. S. Nefedov and S. A. Tretyakov, Radio Sci. **38**, 1101 (2003).